

Generation of spatiotemporal colored noise

J. García-Ojalvo

*Departament d'Estructura i Constituents de la Materia, Universitat de Barcelona, Diagonal 647, E-08028 Barcelona, Spain
and Departament de Física i Enginyeria Nuclear, Universitat Politècnica de Catalunya,
Pau Gargallo 5, E-08028 Barcelona, Spain*

J. M. Sancho

Departament d'Estructura i Constituents de la Materia, Universitat de Barcelona, Diagonal 647, E-08028 Barcelona, Spain

L. Ramírez-Piscina

Departament de Física Aplicada, Universitat Politècnica de Catalunya, Jordi Girona Salgado 31, E-08034 Barcelona, Spain

(Received 18 May 1992)

We develop an algorithm to simulate a Gaussian stochastic process that is non- δ -correlated in both space and time coordinates. The colored noise obeys a linear reaction-diffusion Langevin equation with Gaussian white noise. This equation is exactly simulated in a discrete Fourier space.

PACS: 05.40.+j, 02.50.+s

I. INTRODUCTION

Fluctuations in nonequilibrium statistical mechanics are usually modeled by adding a stochastic term to the macroscopic and deterministic differential equation governing the dynamics of the system under consideration. By doing this one obtains what is called a *stochastic differential equation* or *Langevin equation* [1–6]

$$\frac{\partial \psi}{\partial t} = f([\psi(\mathbf{r}, t)], \nabla^2 \psi) + \eta(\mathbf{r}, t). \quad (1)$$

Here $\psi(\mathbf{r}, t)$ is the relevant variable of the system and the first term on the right-hand side is a deterministic force. $\eta(\mathbf{r}, t)$ is a random force called *noise*, which is usually assumed to be Gaussian, and accounts for either internal degrees of freedom, or fluctuations in the constraints imposed externally on the system. In the first case the noise is called *internal noise*, and typically represents thermal fluctuations. In the second case we have *external noise*, whose properties could be controlled experimentally.

In general, internal noise has been assumed to be *white* to a very good approximation. This means that the value of the random field in a given point at a given time does not depend on its value in other points or at other times:

$$\langle \eta(\mathbf{r}, t) \eta(\mathbf{r}', t') \rangle = 2\epsilon \delta(\mathbf{r} - \mathbf{r}') \delta(t - t'), \quad (2)$$

where ϵ is the *intensity* of the noise and $\langle \rangle$ denotes an average over the probability distribution of the random field.

This approximation is reasonable because internal noise moves much more rapidly than the typical time scales of the system, and acts much more locally than any characteristic length scale. This behavior cannot be ensured in the case of external noises, where one must therefore consider situations in which the correlation of the random field between different points and different times could be nonzero. In these cases, the spectrum of

the noise in both k and ω variables is no longer constant, so one speaks of *colored noise*.

Up to now, very little work has been done on field models with nonwhite noises. Nevertheless, one may think of situations in which not only internal uncorrelated noises, but also external colored ones would have an influence on field systems. An example is the study of diffusion processes under stochastic convective velocity fields [7]. Besides, in the last few years, theoretical studies have indicated the possible existence of a phase transition induced by noise [6, 8], and in fact, a phase transition controlled by the correlation time of an Ornstein-Uhlenbeck noise has been found recently [9] in a time-dependent Ginzburg-Landau model (model *A* in Ref. [2]). Thus similar effects can be expected in the case of a noise also correlated in space. Up to now, however, studies have been directed towards either white noises in field models [2, 3], or colored noises in spatial-independent models [6, 8]. In this last case, some simple nonwhite noises were defined [6, 10]. The most famous example of this sort of noise is the *Ornstein-Uhlenbeck process*, which is Gaussian and has zero mean and a correlation given by

$$\langle \xi(t) \xi(t') \rangle = \frac{\epsilon}{\tau} e^{-\frac{|t-t'|}{\tau}}. \quad (3)$$

Here τ is the *correlation time* of the noise, i.e., a measure of its memory in time. The stochastic differential equation which governs its evolution is [8, 9]

$$\dot{\xi}(t) = -\frac{1}{\tau} \xi(t) + \frac{1}{\tau} \eta(t), \quad (4)$$

where $\eta(t)$ is a white noise following (2) without spatial dependence.

We propose a generalization of this very simple idea to take into account finite correlation in space as well. The simplest stochastic differential equation modeling such a noise is the following linear reaction-diffusion equation

$$\dot{\xi}(\mathbf{r}, t) = -\frac{1}{\tau}(1 - \lambda^2 \nabla^2) \xi + \frac{1}{\tau} \eta(\mathbf{r}, t), \quad (5)$$

where $\eta(\mathbf{r}, t)$ is again a white noise following (2) and λ is the *correlation length* of $\xi(\mathbf{r}, t)$. The parameter τ controls the temporal memory of this process as in Eq. (4). Correlation in space comes from the Laplacian term in (5), which couples the values of the field $\xi(\mathbf{r}, t)$ at different points.

Equation (4) is a (stochastic) linear *ordinary* differential equation, so it is easily integrated. Equation (5) is also a linear but *partial* differential equation, so integration, though possible, is not so simple. One could try to solve the equation by performing the integration numerically using a standard finite-difference scheme, but this is not the best method (see the next section). An alternative procedure is to transform it to Fourier space, simulate it there, and then transform the solution back to real space. This is the procedure we will follow here. At each time step of the integration the variable $\xi(\mathbf{r}, t)$ is generated exactly in the discrete Fourier space and then, if necessary, it will be transformed back into real space.

Section II is devoted to the Fourier-transformed equation and the theoretical results that can be deduced from it. In Sec. III the algorithm is derived. In Sec. IV we present our numerical results and compare them with those derived theoretically. Finally, in Sec. V we present some conclusions and comments.

II. CORRELATED NOISE IN FOURIER SPACE

The stochastic process we want to generate is $\xi(\mathbf{r}, t)$ obeying Eqs. (5) and (2). The discrete versions of these two equations in a periodic square lattice of $L \times L$ cells are

$$\frac{d\xi_{ij}}{dt} = -\frac{1}{\tau}(\delta_{ik}\delta_{jl} - \lambda^2 \nabla_{ijkl}^2) \xi_{kl} + \frac{1}{\tau} \eta_{ij}(t), \quad (6)$$

$$\langle \eta_{ij}(t) \eta_{kl}(t') \rangle = \frac{2\epsilon}{(\Delta x)^2} \delta_{ik} \delta_{jl} \delta(t - t'), \quad (7)$$

where Δx is the spacing of the lattice and all the indexes run from 1 to L . The operator ∇_{ijkl}^2 is a finite-difference approximation to the Laplacian operator. Here we will take [11]

$$\nabla_{ijkl}^2 \xi_{kl} = \frac{1}{(\Delta x)^2} (\xi_{i+1,j} + \xi_{i,j+1} + \xi_{i-1,j} + \xi_{i,j-1} - 4\xi_{ij}). \quad (8)$$

The relationship between the continuum variable \mathbf{r} and the indexes i, j running over the discrete lattice is

$$\mathbf{r} = (x, y) = \Delta x(i, j). \quad (9)$$

First, let us examine the difficulties generated by a standard simulation. A first-order Euler algorithm applied to Eqs. (6) and (7) leads to [7]

$$\begin{aligned} \xi_{ij}(t + \Delta t) &= \xi_{ij}(t) - \frac{\Delta t}{\tau} (\delta_{ik} \delta_{jl} - \lambda^2 \nabla_{ijkl}^2) \xi_{kl} \\ &\quad + \frac{\sqrt{2\epsilon \Delta t}}{\tau \Delta x} \alpha_{ij}(t), \end{aligned} \quad (10)$$

where $\alpha_{ij}(t)$ are Gaussian-independent random numbers of zero mean and variance equal to one. Since this is a first-order algorithm, a very small value of Δt should be taken. Nevertheless, there is a second condition in order to stabilize the contribution of the Laplacian operator ∇^2 [12]:

$$\frac{4\lambda^2}{\tau} \frac{\Delta t}{(\Delta x)^2} < 1. \quad (11)$$

So once the lattice spacing Δx is chosen, the step of integration Δt depends on the parameters λ and τ . This is a strong condition which will lead to an excessive use of computer time in some circumstances. Hence an algorithm whose step of integration does not depend on the parameters $\Delta x, \lambda, \tau$, or ϵ would be desirable. In the following we present a method to accomplish this objective.

In our discrete space we no longer have a partial differential equation, but a system of $L \times L$ coupled ordinary differential equations. To decouple such a system we will work on Fourier space. Let us thus define the Fourier transform of the discrete field ξ_{ij} as

$$\xi_{\mu\nu} = (\Delta x)^2 \sum_{i,j} e^{-i\mathbf{k}\cdot\mathbf{r}} \xi_{ij}. \quad (12)$$

The sum includes all the lattice sites of Eq. (9) and the wave vector \mathbf{k} is given by

$$\mathbf{k} = (k_x, k_y) = \frac{2\pi}{L\Delta x} (\mu, \nu) \quad (13)$$

(greek indexes also run from 1 to L and will be used to denote discrete k variables in Fourier space).

From (12) it can be seen that Eqs. (6) and (7) transform into

$$\frac{d\xi_{\mu\nu}}{dt} = -\frac{1}{\tau} c_{\mu\nu\rho\sigma} \xi_{\rho\sigma} + \frac{1}{\tau} \eta_{\mu\nu}(t), \quad (14)$$

$$\langle \eta_{\mu\nu}(t) \eta_{\mu'\nu'}(t') \rangle = 2\epsilon (L\Delta x)^2 \delta_{\mu,-\mu'} \delta_{\nu,-\nu'} \delta(t - t'), \quad (15)$$

where $c_{\mu\nu\rho\sigma}$ is the Fourier transform of the linear operator $(\delta_{ik} \delta_{jl} - \lambda^2 \nabla_{ijkl}^2)$ appearing in Eq. (6), which is explicitly

$$c_{\mu\nu\rho\sigma} = c_{\mu\nu} \delta_{\mu\rho} \delta_{\nu\sigma}, \quad (16)$$

$$c_{\mu\nu} = 1 - \frac{2\lambda^2}{(\Delta x)^2} \left[\cos\left(\frac{2\pi\mu}{L}\right) + \cos\left(\frac{2\pi\nu}{L}\right) - 2 \right]. \quad (17)$$

We can see that the expected decoupling of the equations (14) now takes place:

$$\frac{d\xi_{\mu\nu}}{dt} = -\frac{1}{\tau} c_{\mu\nu} \xi_{\mu\nu} + \frac{1}{\tau} \eta_{\mu\nu}(t). \quad (18)$$

Notice that as Δx tends to 0 and L tends to ∞ keeping $L\Delta x$ fixed (continuum limit) we have

$$c_{\mu\nu} \longrightarrow \omega(k) = 1 + \lambda^2 k^2. \quad (19)$$

Equation (18) is nothing but a set of *independent* ordi-

nary differential equations for *each* pair of components of the wave vector in Fourier space. It is linear, so it can be easily integrated to obtain the evolution of each Fourier mode.

Formal integration of (18) leads to

$$\xi_{\mu\nu}(t) = \xi_{\mu\nu}(0)e^{-\frac{c_{\mu\nu}}{\tau}t} + \frac{1}{\tau} \int_0^t e^{-\frac{c_{\mu\nu}}{\tau}(t-t')} \eta_{\mu\nu}(t') dt'. \quad (20)$$

From this expression and using (15) and the fact that $c_{\mu\nu}$ is an even function of the wave vector, one can calculate the correlation of the field at equal times:

$$\begin{aligned} \langle \xi_{\mu\nu}(t) \xi_{\mu'\nu'}(t) \rangle &= \langle \xi_{\mu\nu}(0) \xi_{\mu'\nu'}(0) \rangle e^{-\frac{c_{\mu\nu} + c_{\mu'\nu'}}{\tau} t} \\ &+ \frac{\epsilon(L\Delta x)^2}{\tau c_{\mu\nu}} \left(1 - e^{-\frac{2c_{\mu\nu}}{\tau} t} \right) \delta_{\mu, -\mu'} \delta_{\nu, -\nu'}, \end{aligned} \quad (21)$$

where its stationary value is given by

$$\lim_{t \rightarrow \infty} \langle \xi_{\mu\nu}(t) \xi_{\mu'\nu'}(t) \rangle = \frac{\epsilon(L\Delta x)^2}{\tau c_{\mu\nu}} \delta_{\mu, -\mu'} \delta_{\nu, -\nu'}. \quad (22)$$

If the *structure function* is defined by

$$S_{\mu\nu}(t) = \frac{\langle \xi_{\mu\nu}(t) \xi_{-\mu-\nu}(t) \rangle}{(L\Delta x)^2}, \quad (23)$$

then from Eq. (21) we find that

$$S_{\mu\nu}(t) = \left(S_{\mu\nu}(0) - \frac{\epsilon}{\tau c_{\mu\nu}} \right) e^{-\frac{2c_{\mu\nu}}{\tau} t} + \frac{\epsilon}{\tau c_{\mu\nu}} \quad (24)$$

and its stationary value is

$$S_{\mu\nu}^{\text{st}} = \frac{\epsilon}{\tau c_{\mu\nu}}. \quad (25)$$

Transforming this last quantity back to real space gives the *stationary correlation function*:

$$G_{ij}^{\text{st}} = \frac{1}{(L\Delta x)^2} \sum_{\mu, \nu} e^{-i\mathbf{k} \cdot \mathbf{r}} S_{\mu\nu}^{\text{st}}. \quad (26)$$

We can also calculate the stationary correlation in Fourier space at different times:

$$\langle \xi_{\mu\nu}(t) \xi_{\mu'\nu'}(t') \rangle_{\text{st}} = \frac{\epsilon(L\Delta x)^2}{\tau c_{\mu\nu}} e^{-\frac{c_{\mu\nu}}{\tau} |t-t'|} \delta_{\mu, -\mu'} \delta_{\nu, -\nu'}. \quad (27)$$

We can see that this correlation decays with an effective relaxation time $\frac{\tau}{c_{\mu\nu}}$, which is equal to τ only for the $k = 0$ Fourier mode.

At the continuum limit expressions (24) and (25) become

$$S(\mathbf{k}, t) = \left(S(\mathbf{k}, 0) - \frac{\epsilon}{\tau \omega(\mathbf{k})} \right) e^{-\frac{2\omega(\mathbf{k})t}{\tau}} + \frac{\epsilon}{\tau \omega(\mathbf{k})}, \quad (28)$$

$$S_{\text{st}}(\mathbf{k}) = \frac{\epsilon}{\tau \omega(\mathbf{k})}. \quad (29)$$

III. THE ALGORITHM

Here we will develop an iterative algorithm to simulate $\xi_{\mu\nu}$ at a time $t + \Delta t$ from its known value at a time t . Integration of (18) between t and $t + \Delta t$ leads to [see Eq. (20)]

$$\begin{aligned} \xi_{\mu\nu}(t + \Delta t) &= \xi_{\mu\nu}(t) e^{-\frac{c_{\mu\nu}}{\tau} \Delta t} \\ &+ \frac{1}{\tau} e^{-\frac{c_{\mu\nu}}{\tau} \Delta t} \int_t^{t+\Delta t} e^{-\frac{c_{\mu\nu}}{\tau}(t-t')} \eta_{\mu\nu}(t') dt'. \end{aligned} \quad (30)$$

The integral term on the right-hand side of this last expression can be considered as a new random variable $\beta_{\mu\nu}(t)$. This random quantity is also Gaussian and has zero mean. Its variance can be calculated by means of (15)

$$\langle \beta_{\mu\nu}(t) \beta_{\mu'\nu'}(t) \rangle = \frac{\epsilon(L\Delta x)^2}{\tau c_{\mu\nu}} \left(1 - e^{-\frac{2c_{\mu\nu}}{\tau} \Delta t} \right) \delta_{\mu, -\mu'} \delta_{\nu, -\nu'}. \quad (31)$$

Then it can be expressed as [13, 14]:

$$\beta_{\mu\nu} = \sqrt{\frac{\epsilon(L\Delta x)^2}{\tau c_{\mu\nu}} \left(1 - e^{-\frac{2c_{\mu\nu}}{\tau} \Delta t} \right)} \alpha_{\mu\nu}, \quad (32)$$

where $\alpha_{\mu\nu}$ are Gaussian random numbers of correlation

$$\langle \alpha_{\mu\nu} \alpha_{\mu'\nu'} \rangle = \delta_{\mu, -\mu'} \delta_{\nu, -\nu'}. \quad (33)$$

In the Appendix we will give the technical details to simulate Gaussian random numbers with this kind of “anti-correlation.” The algorithm is then

$$\begin{aligned} \xi_{\mu\nu}(t + \Delta t) &= \xi_{\mu\nu}(t) e^{-\frac{c_{\mu\nu}}{\tau} \Delta t} \\ &+ \sqrt{\frac{\epsilon(L\Delta x)^2}{\tau c_{\mu\nu}} \left(1 - e^{-\frac{2c_{\mu\nu}}{\tau} \Delta t} \right)} \alpha_{\mu\nu}. \end{aligned} \quad (34)$$

From (22), the most convenient initial condition is

$$\langle \xi_{\mu\nu}(0) \xi_{\mu'\nu'}(0) \rangle = \frac{\epsilon(L\Delta x)^2}{\tau c_{\mu\nu}} \delta_{\mu, -\mu'} \delta_{\nu, -\nu'}, \quad (35)$$

so that the initial value of the field is chosen as follows:

$$\xi_{\mu\nu}(0) = \sqrt{\frac{\epsilon(L\Delta x)^2}{\tau c_{\mu\nu}}} \alpha_{\mu\nu} \quad (36)$$

with $\alpha_{\mu\nu}$ defined above with correlation (33). This initial condition guarantees the stationarity of the noise from the beginning of the process.

IV. RESULTS

Simulations were performed on an IBM 3090-XA computer with a vector facility. Our square lattice has 64×64 cells. We chose two time steps $\Delta t = 0.05$ and $\Delta t = 1.0$ in order to check the quality of the method and a spacing $\Delta x = 1.0$. Results were analyzed from the beginning of the simulations since, as we have already mentioned, initial condition (36) ensures the immediate attainment of the stationary state. The results we present were averaged over 2500 runs.

In Fig. 1 the inverse of the stationary structure function versus k^2 is shown. Perfect agreement is observed with the result (25) coming from the discrete theory. The continuum result (29) only matches our results when k is small, as expected. The same results are obtained for $\Delta t = 1.0$, which is an indication of the exactness of our method.

In Fig. 2 the correlation function (27) (with $\Delta t = 0.05$) is shown against time difference for different values of $|k|$. As $|k|$ increases, the effective relaxation time decreases according to $\tau_{\text{eff}} = \tau/c_{\mu\nu}$.

Once the stationary structure function has been obtained from the simulation results, the discrete Fourier antitransform can be performed to find the stationary correlation function (26). In Fig. 3 correlation functions for three values of the correlation length are plotted against r . They are all normalized to 1 in $r = 0$ in order to show that a greater correlation length corresponds to a slower decay of the spatial correlation, as expected. Thus, Fig. 3 shows the spatial memory of the noise generated, such as in Fig. 2 the temporal memory is observed.

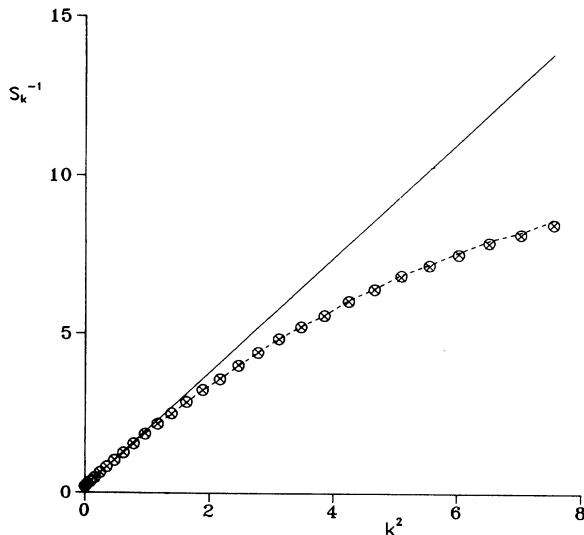


FIG. 1. Inverse of the structure function against k^2 for $\epsilon = 5, \tau = 1$, and $\lambda = 3$. The solid line is the continuum theoretical prediction (29) and the dashed line is the result from the discrete theory (25). Crosses and circles are our simulation results for $\Delta t = 0.05$ and $\Delta t = 1.0$, respectively.

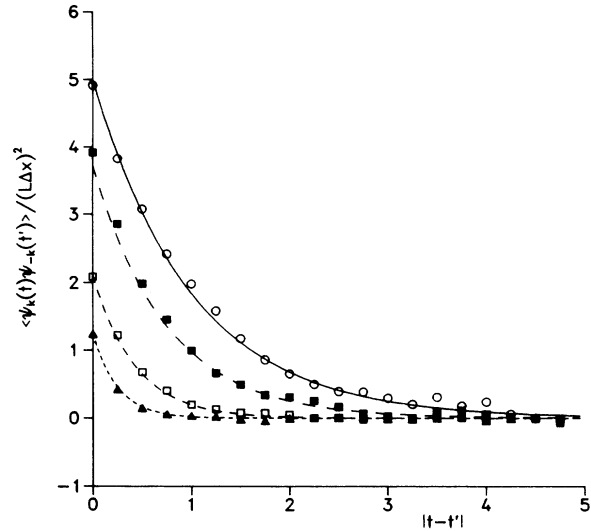


FIG. 2. The time correlation (27) against time difference for different values of k : open circles correspond to the $(0,0)$ wave vector, solid squares to $(0,2)$, open squares to $(0,4)$, and solid triangles to $(0,6)$. The solid and dashed lines correspond to the theoretical results of Eq. (27). The values of the parameters of the noise are the same as those in Fig. 1. Here $\Delta t = 0.05$ has been used.

V. CONCLUSIONS

We have presented an algorithm to generate spatiotemporal Gaussian colored noises defined by an intensity ϵ , a spatial correlation λ , and a temporal correlation τ . This algorithm works in discrete Fourier space, and its main

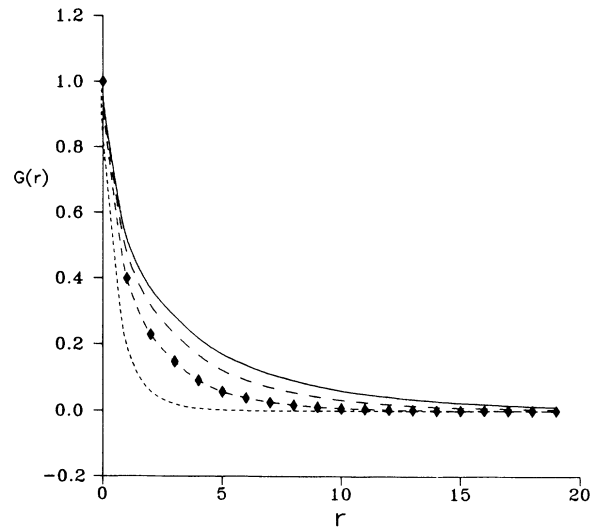


FIG. 3. Normalized correlation function (26) against r for different values of λ . The solid line corresponds to $\lambda = 7$, and the dashed lines to $\lambda = 5, 3, 1$ in decreasing order. The values of the other parameters are ($\epsilon = 5, \tau = 1$, and $\Delta t = 0.05$). The solid diamonds are the simulation results for $\lambda = 3$ using $\Delta t = 1$.

advantage is that it is *exact*. Nevertheless, there is an approximation concerning the spacing Δx when a discrete expression for the Laplacian operator ∇^2 is chosen. If one needs the noise in real space, ξ_{ij} , then a second approximation is necessary, which is involved in the inverse fast Fourier transform of $\xi_{\mu\nu}$. Hence the approximations concern only the transition from continuum to discrete space.

ACKNOWLEDGMENTS

We acknowledge the Direccion General de Investigacion Cientifica y Técnica (Spain) (Project No. PB90-0030) and the European Economic Community [Project No. SC1.0043.C(H)] for financial support.

APPENDIX: DISCRETE FOURIER TRANSFORM OF A REAL FIELD

Here we present a method to generate the $L \times L$ Fourier modes corresponding to an anticorrelated Gaussian process with the appropriate symmetries.

Let us consider a real field ξ_{ij} in a periodic discrete square lattice of $L \times L$ sites. The indexes i, j run, for computational convenience, from 0 to $L - 1$. We define the discrete Fourier transform of such a field by (12), with \mathbf{r} and \mathbf{k} given by (9) and (13), respectively. Now due to the periodic boundary conditions one can easily see that a periodicity relation also holds in Fourier space:

$$\xi_{\mu\nu} = \xi_{\mu+pL, \nu+qL}, \quad (\text{A1})$$

where p and q are integer numbers. Moreover, if ξ_{ij} is real, Eq. (12) leads to the symmetry relation:

$$\xi_{\mu\nu} = \xi_{-\mu, -\nu}^*. \quad (\text{A2})$$

This means that the zero mode in Fourier space is a symmetry center for the real part of the field and an antisymmetry center for the imaginary part. By combining (A1) and (A2) we obtain another symmetry relation:

$$\xi_{\mu\nu} = \xi_{pL-\mu, qL-\nu}^*, \quad (\text{A3})$$

so that not only $k = 0$, but also all points in Fourier space of the form $\frac{1}{2} \left(pL \frac{2\pi}{L\Delta x}, qL \frac{2\pi}{L\Delta x} \right)$ are symmetry points in the sense mentioned above. This is shown in Fig. 4(a), where periodicity is also noticeable. Black sites are the symmetry points already mentioned. The bottom row and right column are *identical* with the top row and left column. In fact, they do not belong to the unitary lattice drawn but to the neighboring ones, which are identical to it. Because of Eq. (A1), sites A_1 , B , and C are exactly the same, and because of Eq. (A3), A_1 and A_2 have the same real part, while their imaginary parts are just of opposite sign. Notice that all these symmetry (black) points have no imaginary part.

In the text $\xi_{\mu\nu}$ and $\eta_{\mu\nu}$ are the Fourier transforms (complex fields, in general) of the real fields ξ_{ij} , η_{ij} , so they verify relation (A2). One can easily see that $\beta_{\mu\nu}$, and therefore $\alpha_{\mu\nu}$, also have these symmetries.

Let us remember that we want to generate a complex

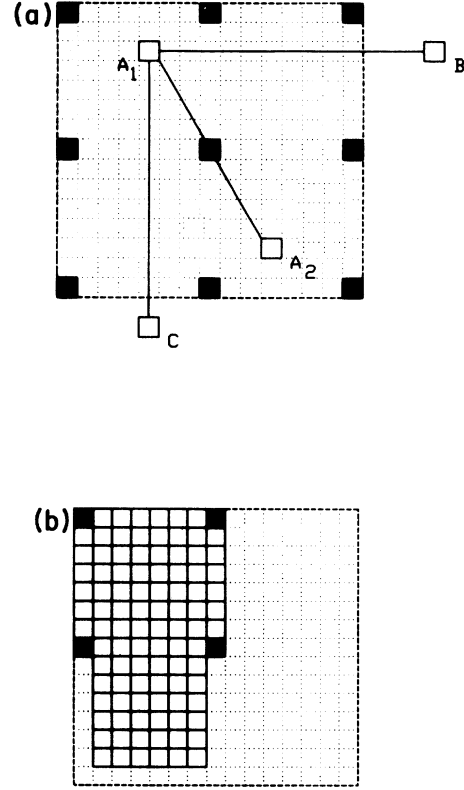


FIG. 4. Symmetry properties of the Fourier variables.

Gaussian random field $\alpha_{\mu\nu}$ with zero mean and correlation given by (33). This is done by constructing $\alpha_{\mu\nu}$ as

$$\alpha_{\mu\nu} = a_{\mu\nu} + ib_{\mu\nu}. \quad (\text{A4})$$

In order to have correlation (33) and because of symmetry relation (A2), these two new (real) Gaussian random fields can be taken to be uncorrelated in space and have zero mean and variance given by

$$\langle a_{\mu\nu}^2 \rangle = \langle b_{\mu\nu}^2 \rangle = \frac{1}{2}, \quad (\text{A5})$$

except in the black sites of Fig. 4(a), where

$$\langle a_{\mu\nu}^2 \rangle = 1, \quad (\text{A6})$$

$$\langle b_{\mu\nu}^2 \rangle = 0.$$

These random numbers are Gaussian and can be obtained in a standard way by means of, for instance, a Box-Mueller algorithm. One can easily see that making use of Eq. (A4) with (A5) and (A6) and considering symmetry relation (A2), correlation (33) is achieved. Moreover, we only need to generate the field $\xi_{\mu\nu}$ and the random numbers $\alpha_{\mu\nu}$ corresponding to the shadowed cells of Fig. 4(b) [the value of the field in the rest of sites is then completely determined by Eq. (A2)]. Notice that the number of independent random quantities which are needed is just $L \times L$, which is the number of variables that we originally wanted to generate in real space.

- [1] C.W. Gardiner, *Handbook of Stochastic Methods* (Springer-Verlag, Berlin, 1983).
- [2] P. Hohenberg and B.I. Halperin, *Rev. Mod. Phys.* **49**, 435 (1977).
- [3] J.D. Gunton, M. San Miguel, and P.S. Sahni, in *Phase Transitions and Critical Phenomena*, edited by C. Domb and J.L. Lebowitz (Academic, New York, 1983), Vol. 8, p. 267, and references therein.
- [4] S. Kai, S. Wakabayashi, and M. Imasaki, *Phys. Rev. A* **33**, 2612 (1986).
- [5] H. Haken, *Laser Light Dynamics* (North-Holland, Amsterdam, 1985).
- [6] W. Horsthemke and R. Lefever, *Noise-Induced Transitions* (Springer-Verlag, Berlin, 1984).
- [7] A. Careta, F. Sagés, J.M. Sancho, and L. Ramírez-Piscina (unpublished).
- [8] J.M. Sancho and M. San Miguel, in *Noise in Nonlinear Dynamical Systems*, edited by F. Moss and P.V.E. McClintock (Cambridge University, Cambridge, 1989), Vol. 1, p. 72, and references therein.
- [9] J. García-Ojalvo, J.M. Sancho, and L. Ramírez-Piscina, *Phys. Lett. A* (to be published).
- [10] J.M. Sancho, M. San Miguel, S. Katz, and J.D. Gunton, *Phys. Rev. A* **26**, 1589 (1982).
- [11] *Handbook of Mathematical Functions*, edited by M. Abramowitz and I.A. Stegun (Dover, New York, 1972).
- [12] W.H. Press, B.P. Flannery, S.A. Teukolsky, and W.T. Vetterling, *Numerical Recipes* (Cambridge University, Cambridge, 1988).
- [13] R.F. Fox, I.R. Gatland, and G. Vemuri, *Phys. Rev. A* **38**, 5938 (1988).
- [14] L. Ramírez-Piscina, J.M. Sancho, F.J. de la Rubia, K. Lindenberg, and G.P. Tsironis, *Phys. Rev. A* **40**, 2120 (1989).